Interpretation of particle pinches and diffusion coefficients in the edge pedestal of DIII-D H-mode plasmas

W. M. Stacey[1] and R. J. Groebner[2]
[1]*Georgia Tech, Atlanta, Georgia 30332, USA*
[2]*General Atomics, San Diego, California 92186, USA*

(Received 27 August 2009; accepted 11 September 2009; published online 15 October 2009)

A procedure is described for evaluating particle pinches to be used in interpreting particle diffusion coefficients from measured density and temperature profiles in the edge pedestal of tokamak plasmas. Application to the interpretation of two DIII-D [J. Luxon, Nucl. Fusion **42**, 614 (2002)]. discharges yields new information about particle pinches and particle diffusion coefficient profiles in the edge pedestal. © *2009 American Institute of Physics*. [doi:10.1063/1.3241698]

I. INTRODUCTION

In two-dimensional transport analyses (e.g., Refs. 1–3) of the edge plasma in tokamaks it is a common practice to determine a particle diffusion coefficient by fitting the measured density profile with a diffusive particle flux model, although sometimes a pinch-diffusive model is used (e.g., Ref. 4). When a purely diffusive model is used, the inferred diffusion coefficient is sometimes quite small ($D \ll 0.1$ m^2/s) in the steep-gradient edge pedestal region. This raises the question of whether the small inferred diffusion coefficient reflects a reduction in the underlying particle diffusive transport mechanism (i.e., a transport barrier) or is an artifact of neglecting an inward pinch in the inference.

Centrally peaked density profiles in edge-fueled tokamak plasmas have been interpreted as evidence of an inward particle pinch since the earliest days of tokamak research in T3.[5,6] The total radial particle flux was represented[7] as a diffusive component plus a convective (pinch) component $\Gamma = -D\nabla n + nV_{\text{pinch}}$, and Ware[8] offered a neoclassical model for a particle pinch of trapped particles proportional to the toroidal electric field E_ϕ. Values of the pinch velocity inferred from density profiles in ASDEX-Upgrade[9] and JET[10] were close to the neoclassical prediction,[8] although inferences of the pinch velocity in DIII-D,[11] TCV[12], and JET[13] without neutral beams were larger than predicted neoclassically, and large inward pinch velocities were inferred in inductively driven discharges in Tore Supra[14] for which $E_\phi = 0$. Clearly mechanisms other than the neoclassical Ware pinch also drive inward pinches in tokamaks, and a variety of other mechanisms have been suggested—thermal diffusion,[15] polarization electric field ExB drift,[15] poloidal rotation,[16] and turbulence.[17] Several authors (e.g., Refs. 18 and 19) have developed procedures for determining pinch velocities and diffusion coefficients from experimental data.

We have developed a somewhat different procedure for inferring the magnitude of the pinch velocity from experimental data. A general expression for the radial particle flux has been developed[20] from the force balance relationship among the radial particle flux in the plasma edge and the rotation velocities, radial and toroidal electric fields, external momentum torques, pressure gradients, etc. This expression can be interpreted as a "pinch-diffusion" relation for the radial particle flux. It was shown[20] that when experimental measurements were used to evaluate the various terms making up the collection of terms identified as the "pinch velocity" and the radial particle flux was determined from integration of the particle continuity equation, that the resulting values of the pressure gradients could be integrated to obtained density profiles in the edge pedestal of H-mode DIII-D plasmas that were in agreement with directly measured values. These observations led to the formal development of a generalized diffusion theory[21] by substitution of the pinch-diffusion relation into the continuity equation.

The purposes of this paper are to extend this and other work to obtain a generalized pinch-diffusion formalism for the interpretation of particle diffusion coefficients from experimental measurements of the density profiles and to apply this formalism to the interpretation of experimental particle diffusion coefficients in the edge pedestal of a couple of DIII-D H-mode discharges. First, the relevant formalism for interpreting particle diffusion in the presence of a particle pinch is developed, and the evaluation of various terms from experimental data is discussed in Sec. II. Then this formalism is applied to the interpretation of the particle diffusion coefficient profiles.

II. A PINCH-DIFFUSION FORMALISM FOR THE INTERPRETATION OF EXPERIMENTAL PARTICLE DIFFUSION COEFFICIENTS

The toroidal and radial components of the momentum balance equation for ion species j can be written as

$$n_j m_j [(\nu_{jk} + \nu_{dj}) V_{\phi j} - \nu_{jk} V_{\phi k}] = n_j e_j E_\phi^A + n_j e_j B_\theta V_{rj} + M_{\phi j} \tag{1}$$

and

$$V_{\phi j} = \frac{1}{B_\theta}\left[E_r + V_{\theta j} B_\phi - \frac{1}{n_j e_j}\frac{\partial p_j}{\partial r} \right], \tag{2}$$

where ν_{dj} is the toroidal angular momentum transfer frequency due to viscosity, inertial forces, atomic physics reactions with neutral atoms, and other "anomalous" processes (justification for representing these processes in this form is

discussed in Ref. 21), E_ϕ^A is the induced electromagnetic field, M_ϕ is the rate of toroidal momentum deposition due to neutral beams or other sources, and the other symbols have their usual meaning. In general, the subscript k represents a sum over other ion species, but in this paper we consider only a single other species (i.e., an "ion-impurity" deuterium plasma with a fully stripped carbon impurity).

Using Eq. (2) to eliminate the toroidal velocities for both species, Eq. (1) may be rewritten as

$$V_{rj} = -\frac{m_j(\nu_{jk}+\nu_{dj})T_j}{(e_jB_\theta)^2}\left[\left(\frac{1}{p_j}\frac{\partial p_j}{\partial r}\right) - \frac{e_j}{e_k}\frac{\nu_{jk}}{(\nu_{jk}+\nu_{dj})}\left(\frac{1}{p_k}\frac{\partial p_k}{\partial r}\right)\right] + V_{rj}^{\text{pinch}}, \tag{3}$$

where

$$V_{rj}^{\text{pinch}} = \frac{1}{e_jB_\theta}\left[-\left(e_jE_\phi^A + \frac{M_{\phi j}}{n_j}\right) + \frac{m_j\nu_{dj}}{B_\theta}(E_r + V_{\theta j}B_\phi) + \frac{m_j\nu_{jk}B_\phi}{B_\theta}(V_{\theta j} - V_{\theta k})\right]. \tag{4}$$

Equation (3) is a consequence of force balance, of course, and specifies that the $V_r \times B_\theta$ force must be balanced by the sum of a force depending on pressure gradients plus other forces not depending on pressure gradients. This force balance must be satisfied for all plasma equilibria over a range of values for the pressure gradients and other terms involved, which implies that the radial particle flux must satisfy a generalized pinch-diffusion relation involving both particle and thermal diffusion of all ion species in the plasma. We note that V_{rj} is a physical velocity, the average fluid radial velocity of the ions of species j, which could in principle be measured. On the other hand, V_{rj}^{pinch} is a normalized collection of forces acting on the ions, but is not a physical velocity.

It may appear that we are not taking full advantage of the available experimental data since the measured carbon toroidal velocity does not explicitly appear in Eq. (4). However, the measured carbon toroidal velocity is employed to determine ν_{dj}, as discussed in Ref. 22 and summarized in the Appendix.

For our purposes in this paper, which are to infer a particle diffusion coefficient for the deuterium ions from a measured density gradient, we consider the above equations for the case of $j=D$, the main deuterium ion species, and $k=C$, a single fully charged carbon species. For this case, the second term in the square bracket in Eq. (3) is small compared to the first term, and this equation can be simplified to the form

$$V_{rj} \simeq -D_j\left(\frac{1}{p_j}\frac{\partial p_j}{\partial r}\right) + V_{rj}^{\text{pinch}}, \tag{5}$$

where D_j represents the collection of terms multiplying the logarithmic pressure gradient.

If the gradient scale lengths of density $L_{nj}=[(1/n_j)\times(\partial n_j/\partial r)]^{-1}$ and temperature $L_{Tj}=[(1/T_j)(\partial T_j/\partial r)]^{-1}$ are known from experiment, and if the radial particle flux n_jV_{rj} can be determined by solving the continuity equation with known external and recycling neutral ionization sources, then Eq. (5) can be used to infer the experimental particle diffusion coefficient

$$D_j^{\text{expt}} = (V_{rj} - V_{rj}^{\text{pinch}})\frac{L_{nj}^{\text{expt}}L_{Tj}^{\text{expt}}}{(L_{nj}^{\text{expt}}+L_{Tj}^{\text{expt}})}, \tag{6}$$

provided that V_{rj}^{pinch} can be determined. With reference to Eq. (4), E_ϕ^A can be determined from the measured loop voltage, M_ϕ can be calculated for neutral beam injection, and the carbon poloidal and toroidal rotation velocities and E_r are measured. This leaves the deuterium poloidal rotation velocity and ν_{dj} to be determined. A perturbation procedure for determining ν_{dj} by solving the deuterium and carbon toroidal momentum equations "backward," using the measured carbon $V_{\phi k}$, is described in Ref. 22 and summarized in the Appendix. The deuterium poloidal velocity $V_{\theta j}$ must be estimated or calculated. The particular formulation of Eq. (4) was chosen from among several possible formulations because the contribution of this unknown $V_{\theta j}$ to the determination of V_{rj}^{pinch} was estimated numerically to be small. The possibility (likelihood) of anomalous transport processes is taken into account in the determination of D_j^{expt} from Eq. (6) and in the determination of ν_{dj} which enters into the determination of V_{rj}^{pinch}.

III. INTERPRETATION OF PARTICLE DIFFUSION COEFFICIENTS IN DIII-D ELMING H-MODE EDGE PEDESTALS

The interpretive scheme described in Sec. II is used to analyze transport in the DIII-D edge pedestal. A procedure for averaging data taken in specific subintervals between edge localized modes (ELMs) over several consecutive inter-ELM periods and fitting those data in a form convenient for analysis has been described in detail in Ref. 23. We have chosen data taken over the subinterval constituting the last 20% of the inter-ELM interval (i.e., the subinterval just before the next ELM—the so-called "80–99" subinterval) so that the effects of the previous ELM will be minimized. Two DIII-D shots—98889 at about 3960 ms and 119436 at about 3250 ms—were examined. Detailed calculations of the thermal transport interpretation of these shots may be found in Ref. 23.

A. Shot 98889

For shot 98889 (LSN, $R=1.75$ m, $a=0.62$ m, $\kappa=1.755$, $\delta=0.135$, $B=-2.01$ T, $I=1.22$ MA, $q_{95}=4.41$, $P_{\text{NB}}=4.9$ MW) the fitted values in the edge pedestal for the experimental density and temperatures are shown in Fig. 1. The calculated neutral particle density[24] is also shown in Fig. 1.

Fits of the experimental rotational velocities and radial electric field are shown in Fig. 2. The measured carbon poloidal rotation velocities are rather small, varying from a few hundred to less than a thousand m/s. Note that the sign convention for V_θ in DIII-D is opposite from the right-hand current convention used in the formalism of this paper, so that

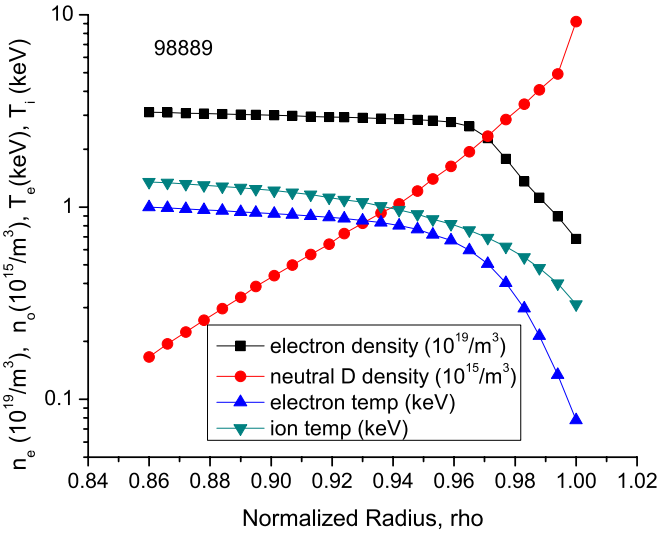

FIG. 1. (Color online) Experimental densities and temperatures for shot 98889.

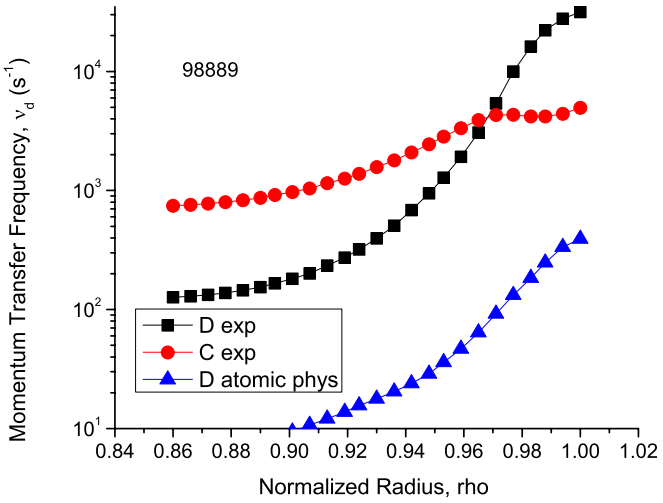

FIG. 3. (Color online) Experimental momentum transfer frequencies and atomic *c-x* contribution.

the (−) experimental values (down at the outboard midplane) reported for the shot are actually used as (+) values in the calculation.

The toroidal angular momentum transfer frequencies inferred from the measured carbon rotation velocity, using the prescriptions in the Appendix, are shown in Fig. 3. Also shown for comparison is the calculated atomic physics (charge exchange, elastic scattering, and ionization) contribution for deuterium.

In Fig. 4, V_{rj}^{pinch} and the various components of the pinch velocity given by Eq. (4) are shown. The radial electric field component was dominant in determining of V_{rj}^{pinch} in this shot. The quantity V_{rj}^{pinch} is referred to as a "pinch" velocity because it is large and inwardly directed (<0) over the outermost radii ($\rho>0.945$), but it is outwardly directed with a magnitude of about 1 m/s for $\rho<0.945$. With respect to Eq. (5), the diffusive component V_{rj}^{diff} must make up the difference between the V_{rj} determined by the continuity equation and V_{rj}^{pinch}. For comparison, the actual radial velocity ($V_{rj}>0$) calculated from the continuity equation, taking into account the neutral beam source and the ionization source of recycling neutrals, is also shown in Fig. 4.

The direct effect of recycling neutrals on the determination of the diffusion coefficient via Eq. (6)—the increase in V_{rj} just inside the separatrix determined from the solution of the continuity equation with a recycling neutral ionization source—is small compared to the effect of the terms in the pinch velocity (in particular E_r), in this and in the other shot considered in this paper. Although this interpretation of the diffusion coefficient from experimental data is a different matter than predicting the edge density profile, this larger magnitude of the pinch velocity than the increase in particle velocity due to neutral recycling is also suggestive of a larger role for the pinch velocity than for the recycling neutrals in determining the edge pedestal density profile, which would

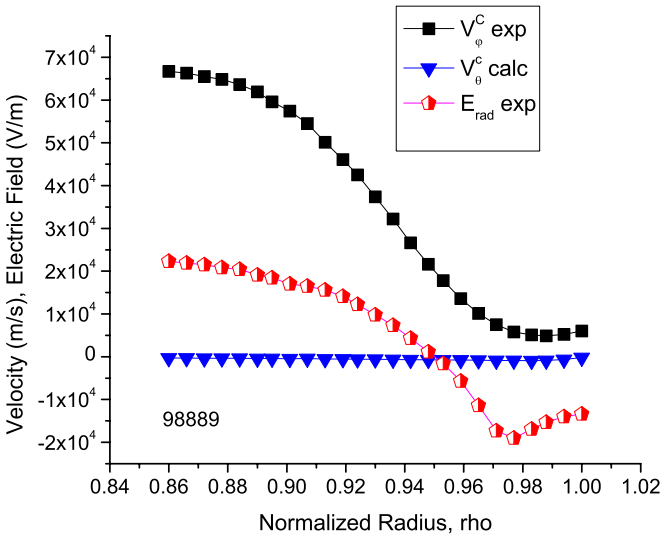

FIG. 2. (Color online) Experimental rotation velocities and radial electric field for shot 98889.

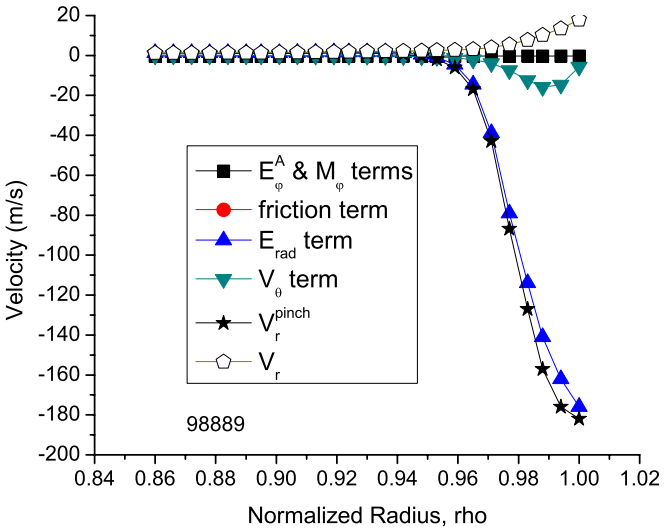

FIG. 4. (Color online) Deuterium radial velocity, pinch velocity, and pinch velocity components.

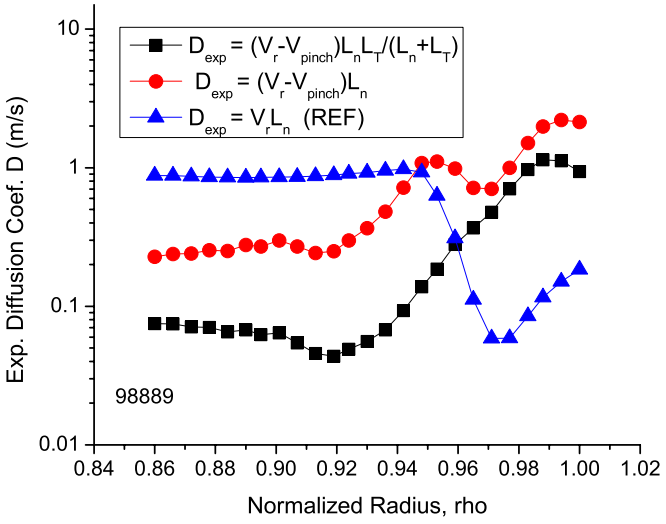

FIG. 5. (Color online) Experimental deuterium particle diffusion coefficients for 98889.

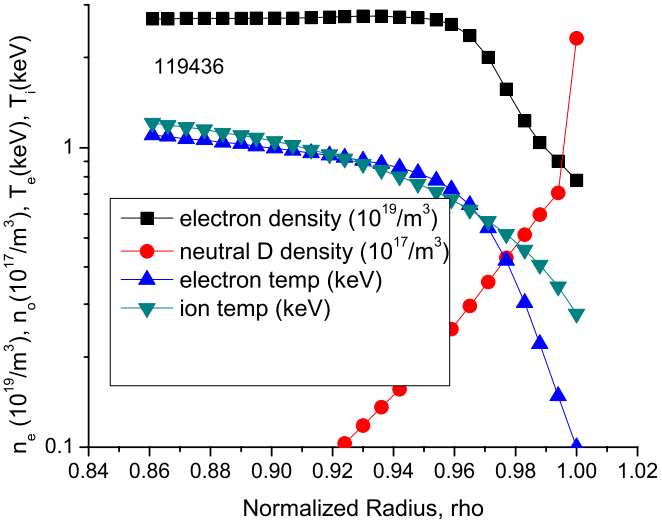

FIG. 6. (Color online) Experimental densities and temperatures for shot 119436.

seem to contradict previous suggestions of the importance of neutral recycling (e.g., Refs. 25 and 26). We plan to make some further investigations along these lines.

The friction term vanishes identically because of the assumption $V_\theta^D = V_\theta^C$ (hidden by the small term due to the E_ϕ and M_ϕ). The experimental deuterium diffusion coefficient interpreted from Eq. (6) is plotted in Fig. 5. For comparison, the usual "pure diffusion" model interpretation of the diffusion coefficient ($D_j^{\text{expt}} = V_{rj} L_{nj}$) is also plotted as the "REF" case. These two interpretations of the diffusion coefficients clearly lead to very different implications for the radial distributions of the underlying transport mechanisms. Also shown for comparison is the diffusion coefficient that would be interpreted by retaining the pinch velocity but neglecting the thermal diffusion [$D_j^{\text{expt}} = (V_{rj} - V_{rj}^{\text{pinch}}) L_{nj}$]. The pure diffusion model ($D_j^{\text{expt}} = V_{rj} L_{nj}$) overpredicts the diffusion coefficient in the core because it fails to account for the outward pinch and underpredicts the diffusion coefficient in the steep gradient region because it fails to account for the large inward pinch.

B. Shot 119436

The fitted values of the experimental density, temperature, rotation, and electric field data in the edge pedestal for H-mode shot 119436 (LSN, $R = 1.77$ m, $a = 0.58$ m, $\kappa = 1.833$, $\delta = 0.44$, $B = -1.64$ T, $I = 1.02$ MA, $q_{95} = 4.20$, and $P_{\text{NB}} = 4.3$ MW) are shown in Figs. 6 and 7. Note that the electron density profile is slightly hollow in the core region.

The toroidal angular momentum transfer frequencies inferred from the measured carbon toroidal rotation velocity are shown in Fig. 8. Also shown for comparison is the calculated atomic physics (charge exchange, elastic scattering, and ionization) contribution to the momentum transfer frequency.

The pinch velocity of Eq. (4) evaluated with the experimental data, using the assumption $V_{\theta D} = V_{\theta C} = V_{\theta C}^{\text{expt}}$, is shown in Fig. 9. Equation (4) was derived from Eq. (1) by using Eq. (2) to eliminate both the deuterium and carbon toroidal rotation velocities. Another form for the pinch velocity which retains an explicit carbon toroidal rotation velocity dependence can be derived by only using Eq. (2) to eliminate the deuterium toroidal rotation velocity in Eq. (1) to obtain instead of Eq. (4),

$$V_{rj}^{\text{pinch}} = \frac{1}{e_j B_\theta}\left[-\left(e_j E_\phi^A + \frac{M_{\phi j}}{n_j} \right) + \frac{m_j(\nu_{jk} + \nu_{dj})}{B_\theta}(E_r + V_{\theta j} B_\phi) - m_j \nu_{jk} V_{\phi k} \right]. \quad (7)$$

This form for V_{rj}^{pinch}, evaluated using $V_{\phi k} = V_{\phi C}^{\text{expt}}$ and $V_{\theta j} = V_{\theta D} = V_{\theta C} = V_{\theta C}^{\text{expt}}$, is also plotted in Fig. 9.

The deuterium particle diffusion coefficients obtained by using the two different forms for V_{rj}^{pinch} in Eq. (6) are plotted in Fig. 10. The very small value of the inferred diffusion coefficient at $\rho \simeq 0.86$ when Eq. (7) is used to evaluate V_{rj}^{pinch} occurs because $V_{rj}^{\text{pinch}} \simeq V_{rj}$ and is probably due to the ap-

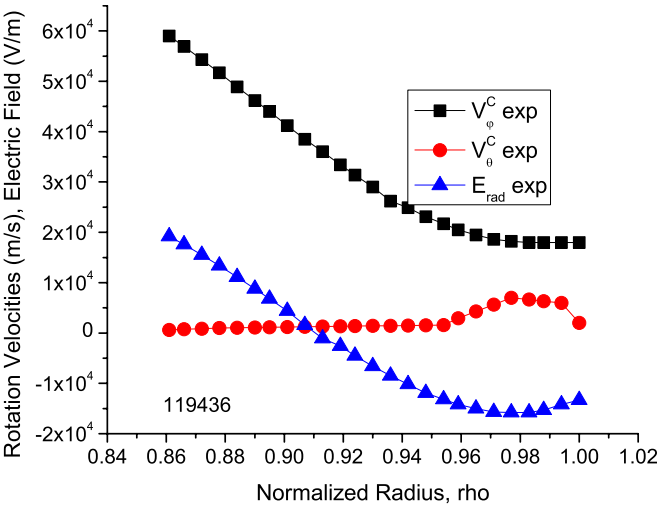

FIG. 7. (Color online) Experimental rotation velocities and radial electric field for shot 119436.

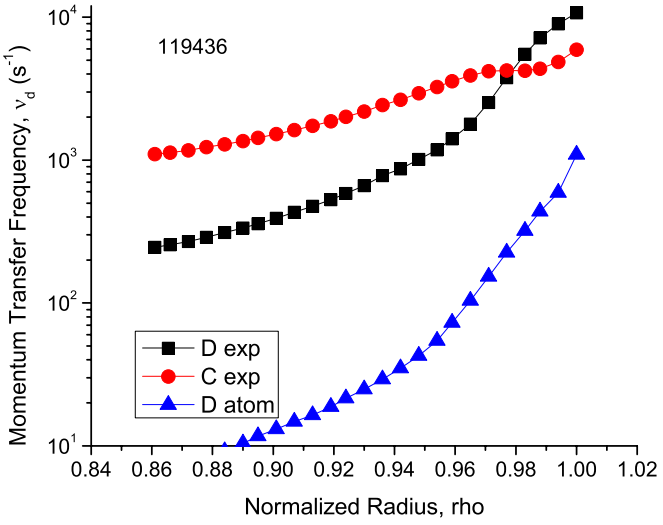

FIG. 8. (Color online) Experimental momentum transfer frequencies and atomic *c-x* contribution.

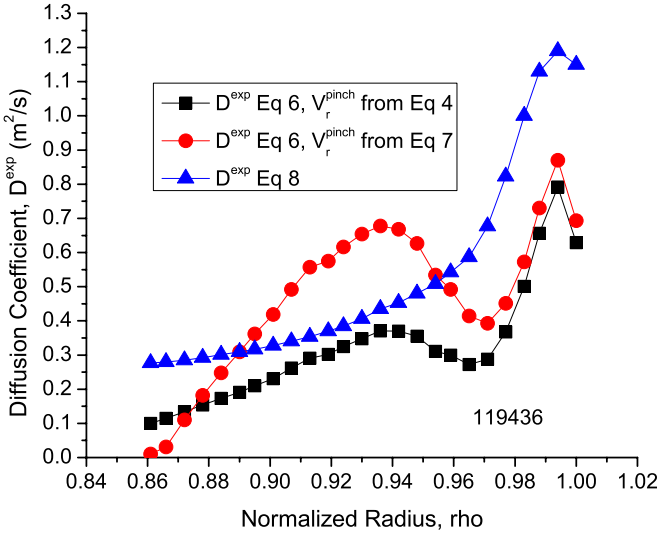

FIG. 10. (Color online) Experimental deuterium particle diffusion coefficients for shot 119436.

proximation $V_{\phi j}=V_{\theta D}=V_{\theta C}=V_{\theta C}^{\text{expt}}$ made in evaluating V_{rj}^{pinch}. Note that the conventional form for a purely diffusive particle flux would yield a negative $D_j^{\text{expt}}=V_{rj}L_{nj}<0$ in the core where the density profile is hollow ($L_{nj}<0$).

When Eq. (2) was used in Eq. (1) to obtain Eqs. (4) and (5), an explicit expression was obtained for the diffusion coefficient in Eq. (5),

$$D_j^{\text{expt}}=\frac{m_j(\nu_{jk}+\nu_{dj})T_j}{(e_jB_\theta)^2}. \tag{8}$$

This expression is interesting in that it differs from the usual neoclassical Pfirsh–Schluter expression by adding to the interspecies momentum transfer frequency due to collisions, (ν_{jk}) the cross-field momentum transfer frequency (ν_{dj}) due to all other processes to obtain a total momentum transfer frequency for species j. Anomalous, atomic physics and neoclassical cross-field momentum transport processes are taken into account via the determination[8] of ν_{dj} from momentum balance using the measured carbon toroidal rotation velocity. Any other anomalous mechanisms that caused a diffusive particle flux in principle could be represented by replacing the classical collision frequency with an effective collision frequency ν_{jk}^{eff}.

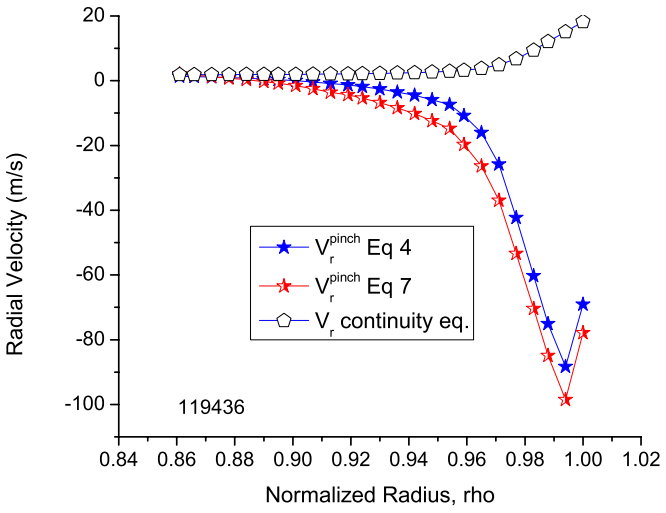

FIG. 9. (Color online) Deuterium radial velocity and pinch velocities for shot 119436.

The experimental diffusion coefficient of Eq. (8), evaluated with ν_{dj} determined from the measured carbon toroidal velocity and the classical ν_{jk}, is also plotted in Fig. 10. There is clearly a dip in the steep gradient region found in interpreting the data with Eq. (5) that is not predicted by Eq. (8) with the classical ν_{jk}. On the other hand, the prediction of Eq. (8) does not depend on the questionable approximation $V_{\theta D}=V_{\theta C}=V_{\theta C}^{\text{expt}}$.

Finally, we make some brief remarks on uncertainties and experiment errors. We have attempted to minimize the effect of random measurement errors by averaging data for a particular time interval between ELMs over several similar inter-ELM periods and to reduce any systematic experimental errors (e.g., by using high time-resolution ion temperature measurements). We examined the calculation for the possibility of numerical errors introduced by, e.g., subtracting large numbers to obtain small results, and found that this did not seem to be a problem (e.g., Fig. 4 shows that the sum and difference of terms leading to the determination of the pinch velocity are dominated by a single term, and this was also the case for the other shot).

IV. SUMMARY

Momentum balance among the electrical, VxB, friction, and pressure gradient forces and the cross-field momentum transfer and external momentum input requires that the radial particle flux satisfies a generalized pinch-diffusion relation. An expression for the pinch velocity can be evaluated using measured quantities, except for the main ion poloidal velocity, which must be estimated. This pinch velocity form can be used together with measured density and temperature profiles to infer the ion particle diffusion coefficient in the edge

pedestal (and in the core). The large inward value of the pinch velocity in the edge pedestal results in the inference of a much larger particle diffusion coefficient than is normally inferred from a purely diffusive model of ion particle transport in the edge pedestal. Experimental and theoretical determination of the main ion poloidal velocity as well as the dominant impurity ion poloidal and toroidal velocities are the principal needs for improvement of this new procedure for the interpretation of particle transport in tokamak edge pedestals.

ACKNOWLEDGMENTS

This work was supported by the U.S. Department of Energy (Grant No. DE-FG02-00-ER54538) with the Georgia Tech Research Corporation and by the U.S. Department of Energy (Contract No. DE-AC03-99ER54463) with General Atomics Co. The authors are grateful to the members of the DIII-D Team who took part in measuring and reducing the data used in this paper. W.M.S. is grateful to General Atomics for its hospitality during the course of this work.

APPENDIX: INFERENCE OF EXPERIMENT TOROIDAL MOMENTUM TRANSFER FREQUENCIES

The results of the derivation in Ref. 22 are summarized here. Solving Eq. (1) for the momentum transfer frequencies for the two plasma species j and k, using a perturbation analysis in the assumed small parameter $(1-V_{\phi j}/V_{\phi k})$, yields to leading order

$$\nu_{dj}=\frac{(n_j e_j E_\phi^A+n_j e_j B_\theta V_{rj}+M_{\phi j})+(n_k e_k E_\phi^A+n_k e_k B_\theta V_{rk}+M_{\phi k})}{(n_j m_j+n_k m_k)V_{\phi k}^{\mathrm{expt}}} \tag{A1}$$

and

$$(V_{\phi j}-V_{\phi k})_0=\frac{(n_j e_j E_\phi^A+n_j e_j B_\theta V_{rj}+M_{\phi j})-n_j m_j \nu_{dj} V_{\phi k}^{\mathrm{expt}}}{n_j m_j(\nu_{jk}+\nu_{dj})}, \tag{A2}$$

and to first order

$$\nu_{dk}=\frac{(n_k e_k E_\phi^A+n_k e_k B_\theta V_{rk}+M_{\phi k})+n_k m_k \nu_{kj}(V_{\phi j}-V_{\phi k})_0}{n_k m_k V_{\phi k}^{\mathrm{expt}}}. \tag{A3}$$

[1] G. D. Porter and DIII-D Team, Phys. Plasmas **5**, 4311 (1998); G. D. Porter, R. Isler, J. Boedo, and T. D. Rognlien, *ibid.* **7**, 3663 (2000).
[2] L. D. Horton, A. V. Chankin, Y. P. Chen, G. D. Conway, D. P. Coster, T. Eich, E. Kaveeva, C. Konz, B. Kurzan, J. Neuhauser, I. Nunes, M. Reich, V. Rozhansky, S. Saarelma, J. Schirmer, J. Schwienzer, S. Voskoboynikov, E. Wolfrum, and ASDEX Upgrade Team, Nucl. Fusion **45**, 856 (2005).
[3] J. D. Callen, R. J. Groebner, J. M. Canick, T. H. Osborne, L. W. Owen, A. Pankin, T. Rafiq, T. D. Rognlien, and W. M. Stacey, "Analysis of pedestal transport," Nucl. Fusion (2009) (to be published).
[4] A. Kallenbach, Y. Andrew, M. Beurskens, G. Corrigan, T. Eich, S. Jachmich, M. Kempenaars, A. Korotkov, A. Loarte, G. Mathtews, P. Monier-Garbet, G. Saibene, J. Spence, W. Suttrop, and JET EFDA Contributors, Plasma Phys. Controlled Fusion **46**, 431 (2004).
[5] L. A. Artsimovich, Plasma Phys. Controlled Nucl. Fusion Res. **2**, 595 (1966).
[6] E. P. Gorbunov, Plasma Phys. Controlled Nucl. Fusion Res. **2**, 629 (1966).
[7] B. Coppi and N. Sharkey, Nucl. Fusion **21**, 1363 (1981).
[8] A. A. Ware, Phys. Rev. Lett. **25**, 916 (1970).
[9] J. Stober, C. Fuchs, O. Gruber, M. Kaufmann, B. Kurzan, F. Meo, H. W. Muller, F. Ryter, and ASDEX Upgrade Team, Nucl. Fusion **41**, 1535 (2001).
[10] M. Valovic, J. Rapp, J. G. Cordey, R. Budny, D. C. McDonald, L. Garzotti, A. Kallenback, M. A. Mahdavi, J. Ongena, Va. Parail, G. Saibene, R. Sartori, M. Stamp, O. Sauter, J. Strachan, W. Suttrop, and EFDA_JET Team, Plasma Phys. Controlled Fusion **44**, 1911 (2002).
[11] D. R. Baker, M. R. Wade, C. C. Petty, M. N. Rosenbluth, T. C. Luce, J. S. deGrassie, B. W. Rice, R. J. Groebner, C. M. Greenfield, E. J. Doyle, C. L. Rettig, T. L. Rhodes, and M. A. Mahdavi, Nucl. Fusion **40**, 1003 (2000).
[12] H. Weisen and E. Minardi, Europhys. Lett. **56**, 542 (2001).
[13] L. Garzotti, *29th EPS Conference on Plasma Physics and Controlled Fusion*, Montreux, 2002 (Institute of Physics, University of Reading, Berkshire, 2002), Vol. 26B, p. 1.035.
[14] G. T. Hoang, C. Bourdelle, B. Pegourie, B. Schunke, J. F. Artaud, J. Bucalossi, F. Clairet, C. Fonzi-Bonizec, X. Garbet, C. Gill, R. Guirlet, F. Imbeaux, J. Lasalle, T. Loarer, C. Lowry, J. M. Travere, E. Tsitrone, and Tore Supra Teams, Phys. Rev. Lett. **90**, 155002 (2003).
[15] R. K. Varma, *Proceedings of the Seventh European Conference on Controlled Fusion and Physics* (EPS, Lausanne, 1975), Vol. 1, p. 10; Plasma Phys. Controlled Fusion **40**, 1999 (1998).
[16] R. J. Taylor, T. A. Carter, J.-L. Gauvreau, P.-A. Gourdain, A. Grossman, D. J. LaFonteese, D. C. Pace, L. W. Schmitz, A. E. White, and T. F. Yates, Nucl. Fusion **45**, 1634 (2005).
[17] F. Jenko, Phys. Plasmas **7**, 514 (2000).
[18] O. Dumbrajs and J. P. T. Koponen, Plasma Phys. Controlled Fusion **40**, 447 (1998).
[19] G. Becker and O. Kardaun, Nucl. Fusion **47**, 33 (2007).
[20] W. M. Stacey, Phys. Plasmas **11**, 4295 (2004); W. M. Stacey and R. J. Groebner, *ibid.* **12**, 042504 (2005).
[21] W. M. Stacey, Contrib. Plasma Phys. **48**, 94 (2008).
[22] W. M. Stacey and R. J. Groebner, Phys. Plasmas **15**, 012503 (2008).
[23] W. M. Stacey and R. J. Groebner, Phys. Plasmas **14**, 122504 (2007).
[24] W. M. Stacey, Nucl. Fusion **40**, 965 (2000).
[25] R. J. Groebner, M. A. Mahdavi, A. W. Leonard, T. H. Osborne, G. D. Porter, R. J. Colchin, and L. W. Owen, Phys. Plasmas **9**, 2134 (2002).
[26] M. A. Mahdavi, R. Maingi, R. J. Groebner, A. W. Leonard, T. H. Osborne, and G. Porter, Phys. Plasmas **10**, 3984 (2003).